

**UNCLASSIFIED**

**AD NUMBER**

**ADB023901**

**LIMITATION CHANGES**

**TO:**

**Approved for public release; distribution is unlimited.**

**FROM:**

**Distribution authorized to U.S. Gov't. agencies only; Test and Evaluation; NOV 1977. Other requests shall be referred to Office of Naval Research, Arlington, VA 22217.**

**AUTHORITY**

**usnrl notice, 4 may 1978**

**THIS PAGE IS UNCLASSIFIED**

THIS REPORT HAS BEEN DELIMITED  
AND CLEARED FOR PUBLIC RELEASE  
UNDER DOD DIRECTIVE 5200.20 AND  
NO RESTRICTIONS ARE IMPOSED UPON  
ITS USE AND DISCLOSURE.

DISTRIBUTION STATEMENT A

APPROVED FOR PUBLIC RELEASE;  
DISTRIBUTION UNLIMITED.

AD B 023901

ION IMPLANTATION OF WIDE  
BANDGAP SEMICONDUCTORS

C.L. Anderson, H.L. Dunlap, C.L. Ramiller, and G.S. Kamath

Hughes Research Laboratories  
3011 Malibu Canyon Road  
Malibu, CA 90265

November 1977

Contract No. N00173-77-C-0051  
Annual Technical Report No. 1  
For Period 1 October 1976 through 30 September 1977

*Reproduction in whole or in part is permitted for any purpose  
of the United States Government.*



Sponsored By  
NAVAL ELECTRONIC SYSTEMS COMMAND  
Department of the Navy  
Washington, D.C. 20360

Monitored By      Distribution limited to U.S. Gov't. agencies only  
NAVAL RESEARCH LABORATORY      test And Evaluation; Other requests  
Department of the Navy      for this document must be referred to  
Washington, D.C. 20375      Dec. 1977

AD No. 1  
DOC FILE COPY

**HUGHES**

HUGHES AIRCRAFT COMPANY  
RESEARCH LABORATORIES

(6) ION IMPLANTATION OF WIDE BANDGAP SEMICONDUCTORS.

(9) Annual Technical Report, No. 1

for Period

1 Oct [REDACTED] — 30 Sep [REDACTED] 77,

(15) CONTRACT NO 173-77-C-0051 *New*

Sponsored by

Naval Electronic Systems Command  
Department of the Navy  
Washington, D.C. 20360

Monitored by

Naval Research Laboratory  
Department of the Navy  
Washington, D.C. 20375

(11) NOV [REDACTED] 77

(12) *440 P.*

ACCESSION NO.	
RTIS	White Section <input type="checkbox"/>
OPC	Buff Section <input checked="" type="checkbox"/>
DATE ACQUIRED	
DISTRIBUTION AVAILABILITY CODES	
BRL	AVAIL, END, or SPECIAL
<i>B</i>	

*Letter on file*

Prepared by

(10) C.L./Anderson, H.L./Dunlap, C.L./Ramiller [REDACTED] G.S./Kamath

172 600

*Mt*

## UNCLASSIFIED

SECURITY CLASSIFICATION OF THIS PAGE (When Data Entered)

REPORT DOCUMENTATION PAGE		READ INSTRUCTIONS BEFORE COMPLETING FORM
1. REPORT NUMBER	2. GOVT ACCESSION NO.	3. RECIPIENT'S CATALOG NUMBER
4. TITLE (and Subtitle) ION IMPLANTATION OF WIDE BANDGAP SEMICONDUCTORS		5. TYPE OF REPORT & PERIOD COVERED Annual Technical Report 1 1 Oct 1977-30 Sep 1977
7. AUTHOR(s) C.L. Anderson, H.L. Dunlap, C.L. Ramiller, and G.S. Kamath		6. PERFORMING ORG. REPORT NUMBER N00173-77-C-0051 <i>new</i>
9. PERFORMING ORGANIZATION NAME AND ADDRESS Hughes Research Laboratories 3011 Malibu Canyon Road Malibu, CA 90265		10. PROGRAM ELEMENT, PROJECT, TASK AREA & WORK UNIT NUMBERS
11. CONTROLLING OFFICE NAME AND ADDRESS Office of Naval Research Department of the Navy Arlington, VA 22217		12. REPORT DATE November 1977
14. MONITORING AGENCY NAME & ADDRESS (if different from Controlling Office) Naval Research Laboratory Department of the Navy Washington, D.C. 20375		13. NUMBER OF PAGES 39
15. SECURITY CLASS (of this report)		
15a. DECLASSIFICATION DOWNGRADING SCHEDULE		
16. DISTRIBUTION STATEMENT (of this Report) Reproduction in whole or in part is permitted for any purpose of the United States government.		
17. DISTRIBUTION STATEMENT (of the abstract entered in Block 20, if different from Report)		
18. SUPPLEMENTARY NOTES		
19. KEY WORDS (Continue on reverse side if necessary and identify by block number) GaAs ion implantation, GaAs encapsulation, GaAs annealing.		
20. ABSTRACT (Continue on reverse side if necessary and identify by block number) The principal dopants studied under this program are sulfur and selenium, both n-type. Topics covered in this report include (1) encapsulation technology, (2) transferability of sulfur or selenium implantation technology, (3) dual implantation of sulfur or selenium with gallium, and (4) thermal conversion of semi-insulating GaAs.		

#### ACKNOWLEDGEMENT

We wish to thank the Electrical Engineering Department and Kellogg Radiation Laboratory of the California Institute of Technology for making their backscattering facilities available for use in these experiments.

## TABLE OF CONTENTS

SECTION	PAGE
1 INTRODUCTION AND SUMMARY . . . . .	7
2 SILICON NITRIDE AND SILICON OXYNITRIDE FILMS FOR ENCAPSULATION OF GaAs . . . . .	9
3 SULFUR TRANSFER TEST S1 . . . . .	30
4 DUAL IMPLANTATION . . . . .	36
5 STUDIES OF THE THERMAL CONVERSION OF SEMI-INSULATING GaAs . . . . .	38
REFERENCES . . . . .	39

## LIST OF ILLUSTRATIONS

FIGURE		PAGE
1	Nomarski photomicrograph near the edge of a non-implanted GaAs sample encapsulated with 2500 Å of Si <sub>3</sub> N <sub>4</sub> at 600°C and annealed at 800°C for 30 min . . . . .	12
2	Nomarski photomicrograph at the center of a non-implanted GaAs sample encapsulated with 2500 Å of Si <sub>3</sub> N <sub>4</sub> at 600°C and annealed at 800°C for 30 min . . . . .	13
3	Film thickness as a function of deposition time for 600°C pyrolytic Si <sub>3</sub> N <sub>4</sub> ; N <sub>2</sub> carrier, 29 liters/min total flow, 0.056% SiH <sub>4</sub> concentration, NH <sub>3</sub> :SiH <sub>4</sub> ratio 110:1 . . . . .	15
4	Growth rate as a function of silane concentration for 600°C pyrolytic Si <sub>3</sub> N <sub>4</sub> ; N <sub>2</sub> carrier, 29 liters/min total flow, NH <sub>3</sub> :SiH <sub>4</sub> ratio $\geq$ 80:1 . . . . .	16
5	Composition of pyrolytic silicon oxynitrides deposited at 600°C using silane, ammonia, and nitrous oxide . . . . .	22
6	Gallium diffusion into Si <sub>0</sub> <sub>x</sub> N <sub>y</sub> and SiO <sub>2</sub> films deposited at 600°C . . . . .	23
7	Comparison of Ga out-diffusion from GaAs as determined by 2MeV <sup>4</sup> He <sup>+</sup> backscattering measurements . . . . .	24

LIST OF TABLES

TABLE	PAGE
1      HRL Results . . . . .	11
2      Characterization of Visible Surface Damage to GaAs and Se-implanted GaAs Substrates Annealed at 800°C in Argon for 30 min . . . . .	17
3      Gallium In-diffusion Results . . . . .	18
4      Electrical Measurements . . . . .	20
5      Physical Appearance of Encapsulated GaAs Samples after a 900°C, 30-min Anneal . . . . .	25
6      Summary of Anneal Studies on GaAs Ingot #3106 . . . .	27
7      Summary of Encapsulant Studies on GaAs Ingot #2988 . .	28
8      Implant Processing for Sulfur Transfer Test "S1" . .	31
9      Composite Results from Sulfur Transfer Test "S1" . .	32
10     Results for Four Implant Conditions Using Pyrolytic SiO <sub>2</sub> Encapsulation and 800°C, 30-min Anneals in Argon . . . . .	34

## SECTION 1

### INTRODUCTION AND SUMMARY

The primary goals of this program are to develop an understanding of the basic physical processes that control the electrical characteristics of ion-implanted layers in GaAs and to exploit the understanding gained to develop a transferable technology for reliable ion-implantation doping of GaAs. During the one-year contract period covered by this report, a major effort was made to study, through duplicate processing and evaluation projects at Hughes Research Laboratories (HRL) and the Naval Research Laboratory (NRL), the factors that affect the transferability and reproducibility of implanting sulfur and selenium into GaAs using  $\text{Si}_3\text{N}_4$  as an annealing encapsulant.

At the outset of this period, neither HRL nor NRL had the capability to deposit the  $\text{Si}_3\text{N}_4$  films required for the transfer tests. Accordingly, both laboratories attempted to develop the required deposition capability. Using Hughes internal funding, we constructed a general-purpose atmospheric-pressure chemical vapor deposition (CVD) system capable of depositing  $\text{Si}_3\text{N}_4$  and a variety of other materials. Adherent, stoichiometric  $\text{Si}_3\text{N}_4$  films have been prepared in this system. Despite their excellent properties as barriers to Ga diffusion, these films have not been successfully used to encapsulate ion-implanted GaAs. We investigated their use in conjunction with pyrolytic  $\text{SiO}_2$ ; we also studied the properties of silicon oxynitrides in several compositions as encapsulants for GaAs. The most successful material at HRL was  $\text{SiO}_2$  prepared by pyrolysis of silane at 390 to  $420^{\circ}\text{C}$ .  $\text{SiO}_2$  prepared by pyrolysis of silane in nitrous oxide at  $600^{\circ}\text{C}$  is considerably superior as a Ga diffusion barrier to the same material deposited at  $420^{\circ}\text{C}$ , and shows some promise as an encapsulant. The results of our studies of encapsulant properties are presented in Section 2.

Before  $\text{Si}_3\text{N}_4$  films were available at either HRL or NRL, we completed a test of the transferability of sulfur implantation into GaAs, using  $\text{Si}_3\text{N}_4$  films supplied by the LFE Corporation, Waltham, MA. This project, performed jointly by HRL and NRL, demonstrated that statistically

equivalent electrical data can be obtained from samples prepared independently at our two laboratories when the same encapsulant is used on all the test samples. The results of this test are summarized in Section 3.

The second area investigated was the use of dual implants (e.g., S+Ga) to correct for implant-induced stoichiometry imbalances, particularly at high implant fluences. We attained a 40% (relative) increase in the electrical activity of selenium implants at the  $10^{14} \text{ cm}^{-2}$  fluence level. No similar increase occurred for sulfur implants. The results of these experiments are summarized in Section 4.

The reliable use of semi-insulating GaAs substrates for ion implantation and device purposes requires that the substrates exhibit high thermal stability. The resistivity of most semi-insulating GaAs material is significantly reduced after high-temperature annealing. NRL has been exploring the possibility of growing high-purity semi-insulating GaAs by the liquid-encapsulated Czochralski (LEC) process. Hughes has developed a simple, reproducible technique for evaluating the thermal stability of GaAs wafers. During this report period we evaluated several samples of the NRL LEC material and samples of material from other sources supplied by NRL. The results of these studies are presented in Section 5.

## SECTION 2

### SILICON NITRIDE AND SILICON OXYNITRIDE FILMS FOR ENCAPSULATION OF GaAs

The use of pyrolytic silicon nitride and silicon oxynitride films as encapsulants for GaAs was examined in some detail. This work was funded both by the present contract and Hughes internal funding. All of this work is summarized here. Briefly, contract funding was used only for deposition evaluation of  $\text{Si}_3\text{N}_4$  films. Internal funding was used in constructing the deposition system and in all work with silicon oxynitrides.

The work reported here involves films deposited in a cold-walled, atmospheric-pressure CVD system. The system is highly automated and helium leak-tight to maximize reproducibility and reduce contamination. The silicon nitride process used in this reactor is similar to that used by MIT Lincoln Laboratories<sup>1</sup> in the sense that the films are deposited by pyrolysis of silane and ammonia and the sample temperature is raised rapidly to the 600 to 700°C range for deposition. In contrast to the Lincoln Labs system (which employs a strip heater), our system uses an rf-heated susceptor on which we have simultaneously encapsulated as many as 40 typical GaAs samples (roughly 7 mm x 7 mm). The temperature of the susceptor can be raised from 400°C to 700°C in less than 10 sec. Using this system, we have successfully deposited  $\text{Si}_3\text{N}_4$  using nitrogen and argon as carrier gases and  $\text{SiO}_2$  and  $\text{SiO}_{x,y}$  using a nitrogen carrier. The resulting films have been analyzed using Rutherford backscattering (RBS) and Auger electron spectroscopy to determine thickness, stoichiometry, and the presence of contaminants. The  $\text{Si}_3\text{N}_4$  films grown using a nitrogen carrier were stoichiometric and free of oxygen and other impurities.  $\text{Si}_3\text{N}_4$  films grown using an argon carrier, however, contained approximately 9% oxygen (apparently because oxygen was present in the in-house argon supply) but were free of other impurities. All work reported below involved films prepared with nitrogen carrier gas.

The first test of our  $\text{Si}_3\text{N}_4$  films for encapsulating ion implants into GaAs used films roughly 3000 Å thick. These films were applied to wafers implanted with selenium (overall implant  $5 \times 10^{12} \text{ cm}^{-2}$  260 keV  $\text{Se}^+$ , at room temperature or  $250^\circ$ ; corner contacts:  $5 \times 10^{14} \text{ cm}^{-2}$  20 keV  $\text{S}^+$ ,  $5 \times 10^{14} \text{ cm}^{-2}$  140 keV  $\text{S}^+$  at room temperature). These samples were intended to be used in a test of the transferability of the selenium ion implantation process in GaAs (transfer test "Se 1").<sup>2</sup> After annealing of these samples at  $800^\circ\text{C}$ , Hall-effect measurements indicated that the electrical properties of the implanted layers were extremely variable (see Table 1). Because of these problems, the transferability of this process was not evaluated. Visual examination of the wafer surfaces revealed easily visible striped patterns. These were initially believed to result either from incomplete removal of the encapsulant or from localized etching of the wafer surface during encapsulant removal. Accordingly, one sample (128) was treated further by removing the Ohmic contacts with HCl, soaking in HF to remove any residual  $\text{Si}_3\text{N}_4$ , and reapplying the Ohmic contacts. Neither the optical nor electrical properties of the sample were changed significantly. Four additional samples (123, 124, 126, 127) were treated further simply by removing and reapplying the contacts. Two of these samples exhibited minor changes in properties after this treatment. The sheet resistance of one sample (127) nearly doubled with no change in sheet carrier concentration. This is not particularly remarkable since the electrical asymmetry of the sample was high (resistance ratio  $\approx 300-400$ ). Sample 126 dramatically increased in asymmetry after this process (resistance ratio change from 240 to  $4 \times 10^4$ ). Apparently, the treatment of this sample destroyed one of the corner contacts.

These results indicated that the appearance of the sample was not the result of residual encapsulant on the surface. Although we had not seen any evidence of stress-related effects in our experiments with unimplanted wafers, we attributed the stripe patterns observed on the samples to damage caused by stress in the nitride coating. As shown in Figures 1 and 2, the damage typically consists of perpendicular cracks or ridges over the face of the  $<100>$  slice. Stoichiometric

Table 1. HRL Results  
Selenium Transfer Test "Se 1", 800° Anneal

Implant Temperature, °C	Die Number	Sheet Resistivity, (Ω/□)	Hall Electron Mobility cm² V⁻¹ sec⁻¹	Sheet Electron Concentration, cm⁻²	Resistance Ratio
20 (Nominal)	123	469	3960	$3.4 \times 10^{12}$	4.3
	123 <sup>a</sup>	453	4250	$3.2 \times 10^{12}$	1.6
	124 <sup>c</sup>	$2.3 \times 10^7$	-14.2	$-1.9 \times 10^{10}$	$4 \times 10^6$
	124 <sup>a,c</sup>	$2.6 \times 10^7$	-0.29	$-8.3 \times 10^{11}$	$2 \times 10^5$
	126 <sup>c</sup>	$3.2 \times 10^7$	-0.89	$-2.2 \times 10^{11}$	240
	126 <sup>a,c</sup>	$1.5 \times 10^7$	-10.6	$-3.9 \times 10^{10}$	$4 \times 10^4$
	127	654	3140	$3.0 \times 10^{12}$	370
	127 <sup>a</sup>	1210	1720	$3.0 \times 10^{12}$	270
	128	1000	2400	$2.6 \times 10^{12}$	160
	128 <sup>b</sup>	1070	2630	$2.2 \times 10^{12}$	78
	129 <sup>a</sup>	$2.3 \times 10^8$	22.0	$1.2 \times 10^9$	2.4
	130 <sup>a</sup>	$4.7 \times 10^7$	12.3	$1.1 \times 10^{10}$	19
250	133 <sup>a</sup>	8590	832	$8.7 \times 10^{11}$	15
	134 <sup>a</sup>	330	1480	$1.3 \times 10^{13}$	9.2
	135 <sup>a</sup>	5300	173	$6.8 \times 10^{12}$	$3 \times 10^4$
	136 <sup>d</sup>	370	3240	$5.2 \times 10^{12}$	1.4
	137 <sup>a</sup>	$1.6 \times 10^8$	10.4	$3.7 \times 10^9$	9.6
	138	263	2440	$9.7 \times 10^{12}$	190
	139 <sup>a</sup>	$9.0 \times 10^6$	53.8	$1.3 \times 10^{10}$	$1 \times 10^6$
	140	216	3960	$7.3 \times 10^{12}$	2.5
20 (Control)	131	$1.7 \times 10^5$	-54.0	$-6.8 \times 10^{11}$	30
	132	$1.2 \times 10^5$	-82.1	$-6.2 \times 10^{11}$	1.2
250 (Control)	141 <sup>a</sup>	$1.6 \times 10^7$	2.91	$1.4 \times 10^{11}$	360
	142 <sup>a</sup>	$2.0 \times 10^7$	19.5	$1.6 \times 10^{10}$	1.1

<sup>a</sup>Remeasured after contact removal with HCl and then reapplied.

<sup>b</sup>Remeasured after contacts removed with HCl, HF soak, and contact reapplication.

<sup>c</sup>Measurement problems encountered (negative resistance or large drifts).

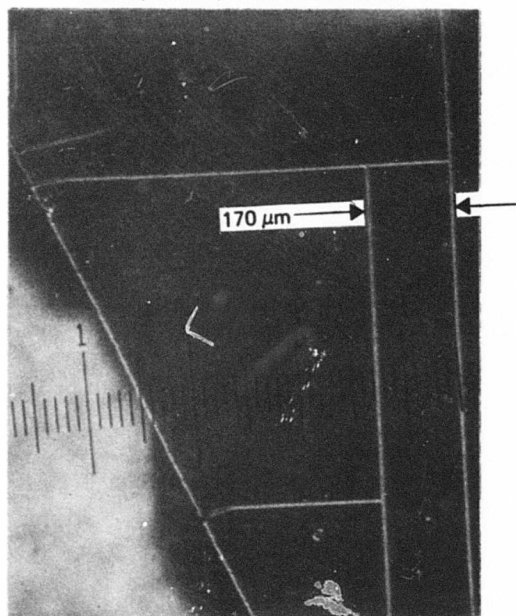
<sup>d</sup>Sample prepared with different coating sequence.

6441-3

NONIMPLANTED GaAs

2500 Å Si<sub>3</sub>N<sub>4</sub> (600°C, 180 Å/min)

800°C, 30 min, ARGON ANNEAL



NOMARSKI PHOTOMICROGRAPH  
75X, 22.4? μm/SMALL DIVISION

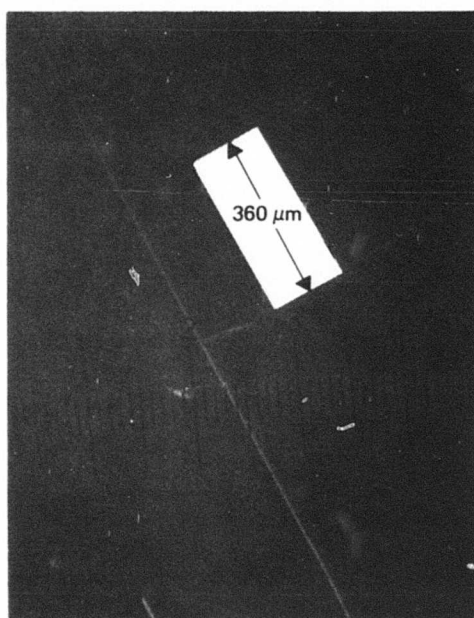
Figure 1. Nomarski photomicrograph near the edge of a nonimplanted GaAs sample encapsulated with 2500 Å of Si<sub>3</sub>N<sub>4</sub> at 600°C and annealed at 800°C for 30 min.

6441-4

NONIMPLANTED GaAs

2500 Å Si<sub>3</sub>N<sub>4</sub> (600°C, 180 Å/min)

800°C, 30 min ARGON ANNEAL



NOMARSKI PHOTOMICROGRAPH  
75X, 22.42 μm/SMALL DIVISION

Figure 2. Nomarski photomicrograph at the center of a nonimplanted GaAs. Sample encapsulated with 2500 Å of Si<sub>3</sub>N<sub>4</sub> at 600°C and annealed at 800°C for 30 min.

$\text{Si}_3\text{N}_4$  films deposited by pyrolysis of silane and ammonia are under high tensile stress, which is intrinsic and not due to thermal mismatch.<sup>3</sup> Since this stress varies with deposition parameters, we carefully characterized  $\text{Si}_3\text{N}_4$  deposition in our CVD system.<sup>4</sup> We began with our 600°C  $\text{Si}_3\text{N}_4$  process since at this temperature there is usually no obvious deterioration of the back of the dice from crystal decomposition during nitride deposition. Figure 3 gives film thickness as a function of deposition time at 600°C for the same total gas flow, silane concentration, and ammonia concentration used last quarter to deposit  $\text{Si}_3\text{N}_4$  at 700°C. The scatter presumably results because (1) we do not have mass flow controllers for the system, and (2) nonuniformities in gas flow and susceptor temperature produce noticeable variation in film thickness across most wafers. Figure 4 shows growth rate as a function of silane concentration at 600°C with constant total flow and ammonia concentration. In all cases, the  $\text{NH}_3:\text{SiH}_4$  ratio was well above the 10:1 ratio required to produce stoichiometric  $\text{Si}_3\text{N}_4$  at these temperatures.<sup>3</sup> At a given deposition temperature, the intrinsic stress in the film can be lowered by reducing the growth rate.<sup>3</sup>

The second test of our pyrolytic  $\text{Si}_3\text{N}_4$  films for implant encapsulation used samples implanted with  $1 \times 10^{13} \text{ cm}^{-2}$   $\text{Se}^+$  implanted at 260 keV and ambient temperature.<sup>4</sup> All samples received contact pads of  $5 \times 10^{13} \text{ cm}^{-2}$   $\text{Se}^+$  at 220 keV. Several dice were reserved as control samples after this step and were not given the overall implant. The dice were processed in batches of six for each encapsulation procedure (four test dice and two control samples per batch). Each batch was treated with a different encapsulant process. The silicon nitride used in this study was deposited at growth rates between 30 Å/min and 180 Å/min. The films used for transfer test "Se 1" were deposited at 700°C at a rate of 1000 Å/min. Consequently, the stress levels in these films should be considerably lower than those used for test "Se 1". All dice were processed identically with regard to cleaning, annealing, and measurement procedures. Annealing was performed in titanium-gettered argon for 30 min at 800°C.

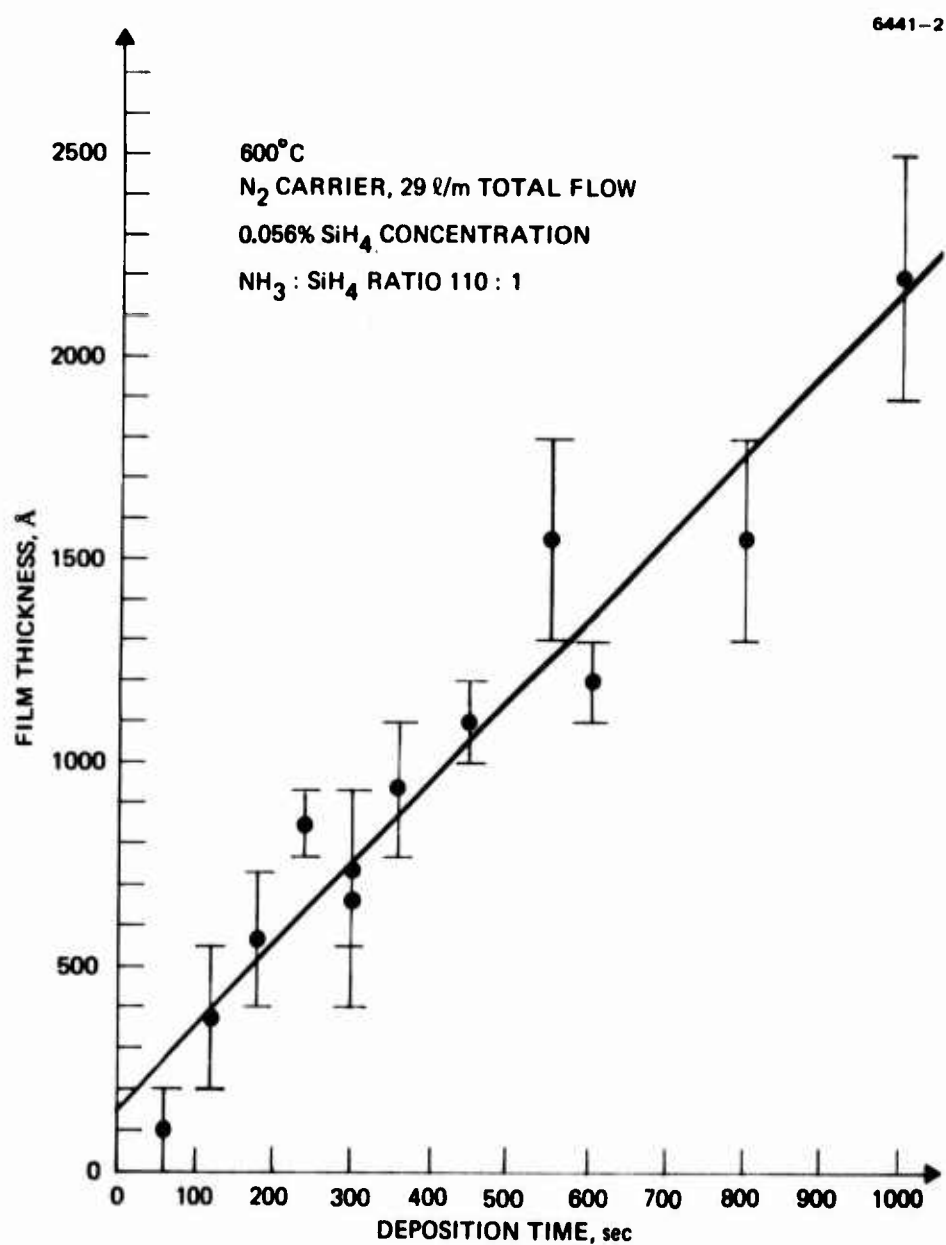


Figure 3. Film thickness as a function of deposition time for 600°C pyrolytic Si<sub>3</sub>N<sub>4</sub>; N<sub>2</sub> carrier, 29 liters/min total flow, 0.056% SiH<sub>4</sub> concentration, NH<sub>3</sub>:SiH<sub>4</sub> ratio 110:1.

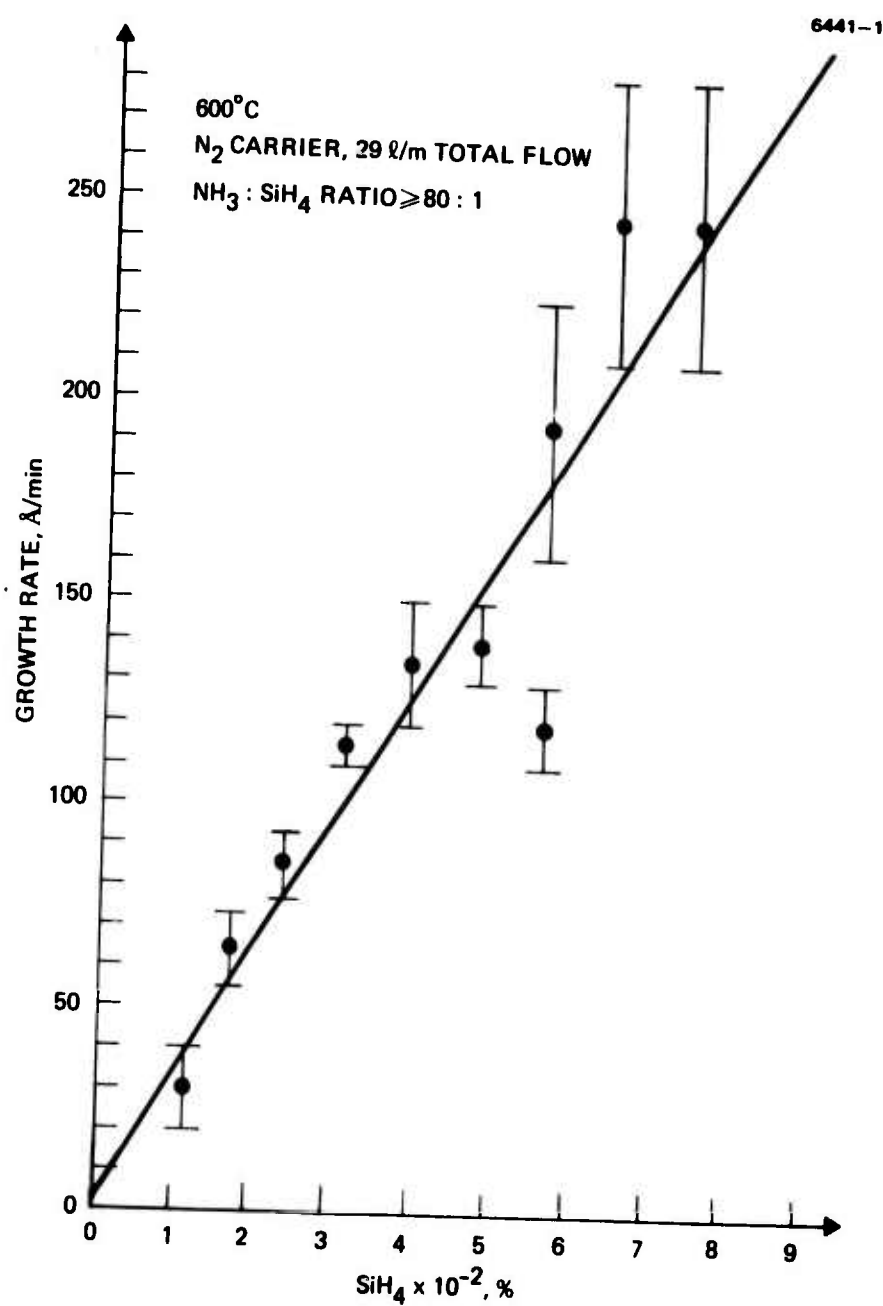


Figure 4. Growth rate as a function of silane concentration for  $600^\circ\text{C}$  pyrolytic  $\text{Si}_3\text{N}_4$ ;  $\text{N}_2$  carrier, 29 liters/min total flow,  $\text{NH}_3 : \text{SiH}_4$  ratio  $\geq 80:1$ .

Table 2 summarizes the results of experiments done so far to determine whether surface damage could be eliminated by changing deposition parameters. Unimplanted GaAs and Se-implanted GaAs were coated with various encapsulants and then annealed at 800°C in argon for 30 min. None of the SiO<sub>2</sub> films caused any visible damage. This is consistent with the hypothesis that the problem is stress related. SiO<sub>2</sub> films deposited on Si are typically under a tensile stress of 1 to  $4 \times 10^9$  dyn/cm<sup>2</sup> (Ref. 5,6), although Si<sub>3</sub>N<sub>4</sub> films on Si are under a tensile stress of 0.5 to  $1.5 \times 10^{10}$  dyn/cm<sup>2</sup> (Ref. 3). The thicker (2200 to 2500 Å) Si<sub>3</sub>N<sub>4</sub> films caused visible damage to GaAs samples whether or not implanted, even when an oxide-coated interface was used. The structures that seem to have the most promise are (1) very thin (~200 Å) Si<sub>3</sub>N<sub>4</sub> films over the implant followed by SiO<sub>2</sub> on both sides of the samples, (2) oxynitrides, and (3) very thin SiO<sub>2</sub> followed by thin Si<sub>3</sub>N<sub>4</sub> over the implant and then by SiO<sub>2</sub> on both sides. We believe that the thick Si<sub>3</sub>N<sub>4</sub> layer on top of the thin oxide was responsible for the damage observed in batch E.

Table 2. Characterization of Visible Surface Damage to GaAs and Se-implanted GaAs Substrates Annealed at 800°C in Argon for 30 min

Batch	Encapsulation	Not Implanted	Se-Implanted
A	SiO <sub>2</sub> , HRL-EB, 3000 Å	No damage	No damage
B	SiO <sub>2</sub> , HRL-II, 2700 Å, 400°C	No damage	No damage
C	Si <sub>3</sub> N <sub>4</sub> , 2500 Å, 600°C, 180 Å/min on the front, then SiO <sub>2</sub> , 2500 Å, 390°C both sides	Damaged	Damaged
D	Si <sub>3</sub> N <sub>4</sub> , 200 Å, 600°C, 30 Å/min on the front, then SiO <sub>2</sub> , 2500 Å, 390°C both sides	No damage	No damage
E	SiO <sub>2</sub> , HRL-II, 200 Å, 390°C, under Si <sub>3</sub> N <sub>4</sub> , 2200 Å, 600°C, 130 Å/min on the front, then SiO <sub>2</sub> , 2500 Å, 390°C both sides	Damaged	Damaged
F	Si <sub>3</sub> N <sub>4</sub> , 500 Å, 600°C, 180 Å/min on the front, then SiO <sub>2</sub> , 2500 Å, 410°C both sides	No damage	No damage

Table 3 presents the results of gallium in-diffusion experiments performed under internal funding. Films of  $\text{Si}_3\text{N}_4$ ,  $\text{SiO}_2$ ,  $\text{SiO}_{x,y}$ ,  $\text{Si}_3\text{N}_4$  over  $\text{SiO}_2$ , and  $\text{SiO}_2$  over  $\text{Si}_3\text{N}_4$  were deposited in our pyrolytic CVD system (denoted HRL-II). The  $\text{Si}_3\text{N}_4$  films were stoichiometric and did not contain any oxygen detectable by RBS or AES. Additional samples of  $\text{SiO}_2$  on Si were prepared at Hughes Torrance Research Center (TRC) and in another CVD system at HRL (denoted HRL-EB). One of the TRC samples was "densified" by annealing in  $\text{O}_2$  at  $1000^\circ\text{C}$ . All of the samples were submerged under gallium in a carbon boat and annealed at  $800^\circ\text{C}$  in a clean argon atmosphere. After cooling, the samples were washed in HCl to remove any gallium on the surface. Backscattering analysis was then performed to determine the concentration and distribution of gallium in the films.

Table 3. Gallium In-diffusion Results

Films Deposited	Result of RBS Measurements
$\text{SiO}_2$ , HRL-EB, $3300 \text{ \AA}$	Ga diffused throughout the film. Highest concentration was in the top one third.
$\text{SiO}_2$ , TRC, $1200 \text{ \AA}$	Ga diffused throughout the film. Concentration was fairly uniform.
$\text{SiO}_2$ , TRC, $1500 \text{ \AA}$ "densified"	No Ga diffusion.
$\text{SiO}_2$ , HRL-II, $3000 \text{ \AA}$ , $380^\circ\text{C}$	Ga diffused throughout the film. Highest concentration was in the top one third.
$\text{SiO}_2$ , $1100 \text{ \AA}$ , $390^\circ\text{C}$ under $\text{Si}_3\text{N}_4$ , $550 \text{ \AA}$ , $640^\circ\text{C}$	No Ga diffusion.
$\text{Si}_3\text{N}_4$ , $650 \text{ \AA}$ , $640^\circ\text{C}$ under $\text{SiO}_2$ , $1100 \text{ \AA}$ , $390^\circ\text{C}$	Ga diffused into the $\text{SiO}_2$ as far as the $\text{SiO}_2/\text{Si}_3\text{N}_4$ interface.
$\text{Si}_3\text{N}_4$ , $1250 \text{ \AA}$ , $700^\circ\text{C}$	No Ga diffusion.
$\text{SiO}_{1.8}\text{N}_{0.5}$ , $2000 \text{ \AA}$ , $680^\circ\text{C}$	Ga diffused throughout the film. Concentration was the highest of this group of samples.

Note: Si substrates, annealed under gallium at  $800^\circ\text{C}$  for 30 min.

Only two effective diffusion barriers were identified during this study:  $\text{Si}_3\text{N}_4$  and "densified"  $\text{SiO}_2$ . Although the latter barrier would not be practical for use on GaAs unless the densification temperature could be lowered, it does demonstrate that a dense  $\text{SiO}_2$  film can block gallium diffusion. The poorest diffusion barrier in the group was an oxygen-rich oxynitride of approximate composition  $\text{SiO}_{1.8}\text{N}_{0.5}$ . Because GaAs diffuses through a layer of  $\text{SiO}_2$  and then stops at an  $\text{Si}_3\text{N}_4$  layer, we also decided to try a thin  $\text{SiO}_2$  film as an interface between the GaAs and the  $\text{Si}_3\text{N}_4$  in the hope that it would reduce the stress on the surface and perhaps saturate with a small amount of gallium.

Table 4 summarizes the electrical properties of the Se-implanted samples as a function of encapsulant treatment, indicating the average and standard deviation of the electrical measurements. All of the dice are from the same ingot: Cr-doped semi-insulating GaAs No. 2988 from Crystal Specialties. These results show that interface contact with even the thinnest nitride layer (200 Å) is sufficient to strain the surface and decrease carrier mobility. As suggested by the  $\text{SiO}_2$ -encapsulated control dice, there may be a residual doping level in this material that would interfere with experiments at low fluence levels but not with encapsulant comparisons.

Since the results with stoichiometric  $\text{Si}_3\text{N}_4$  films were disappointing, our most recent investigations have concentrated on determining the effects of oxygen contamination on the encapsulant properties of our films. Internally funded investigation of the dielectrics (for possible use on GaAs) has given us the capability to deposit  $\text{SiO}_{x,y}\text{N}_y$  films at 600°C with control of the oxygen content. This allows studying the effect of oxygen in the films on Ga in-diffusion from a melt, Ga out-diffusion from GaAs substrates, and the electrical properties of Se-implanted GaAs.

The deposition process uses a mixture of silane, ammonia, and nitrous oxide; this process and the properties of the films produced have been studied previously.<sup>7,8</sup> For the samples used in this study, a total  $\text{N}_2$  carrier gas flow of 30 liters/min was used with the silane and ammonia flows held constant at 11  $\text{cm}^3/\text{min}$  and 6 liter/min, respectively;

Table 4. Electrical Measurements

Batch	Encapsulation	Sheet Resistivity, $\Omega/\square$	Hall Electron Mobility, $\text{cm}^2/\text{V}\cdot\text{sec}$	Sheet Electron Concentration, $\text{cm}^{-2}$
A - implanted	SiO <sub>2</sub> , HRL-EB, 3000 Å	454 ± 32	3360 ± 270	(4.10 ± 0.18) × 10 <sup>12</sup>
- control		1520 ± 180	4036 ± 93	(1.03 ± 0.14) × 10 <sup>12</sup>
B - implanted	SiO <sub>2</sub> , HRL-II, 2700 Å,	402 ± 40	3210 ± 350	(4.88 ± 0.17) × 10 <sup>12</sup>
- control	400°C	980 ± 160	4130 ± 210	(1.57 ± 0.34) × 10 <sup>12</sup>
C - implanted <sup>a</sup>	Si <sub>3</sub> N <sub>4</sub> , 2500 Å, 600°C, 180 Å/min on the front, then SiO <sub>2</sub> , 2500 Å, 390°C on both sides	(4 ± 4) × 10 <sup>8</sup> (1.4 ± 0.6) × 10 <sup>8</sup>	91 ± 77 238 ± 68	(1.3 ± 1.7) × 10 <sup>9</sup> (2.4 ± 1.6) × 10 <sup>7</sup>
D - implanted	Si <sub>3</sub> N <sub>4</sub> , 200 Å, 600°C, 30 Å/min on the front, then SiO <sub>2</sub> , 2500 Å, 390°C on both sides	1020 ± 260 (5.7 ± 1.2) × 10 <sup>8</sup>	2370 ± 670 682 ± 76	(2.70 ± 0.10) × 10 <sup>12</sup> (1.65 ± 0.18) × 10 <sup>7</sup>
E - implanted <sup>a</sup>	SiO <sub>2</sub> , HRL-II, 200 Å, 390°C, under Si <sub>3</sub> N <sub>4</sub> , 2200 Å, 600°C, 130 Å/min on the front, then SiO <sub>2</sub> , 2500 Å, 390°C on both sides	(2.91 ± 1.5) × 10 <sup>8</sup> (1.7 ± 0.5) × 10 <sup>8</sup>	160 ± 80 164 ± 53	(2.9 ± 3.7) × 10 <sup>8</sup> (2.6 ± 1.5) × 10 <sup>8</sup>
F - implanted	Si <sub>3</sub> N <sub>4</sub> , 500 Å, 600°C, 180 Å/min on the front, then SiO <sub>2</sub> , 2500 Å, 410°C on both sides	(1.4 ± 0.9) × 10 <sup>4</sup> 6.00 × 10 <sup>7</sup>	140 ± 190 14.45	(4.6 ± 3) × 10 <sup>12</sup> 7.12 × 10 <sup>9</sup>

Note: aVisible disruption of implanted surface.

bOnly one sample available.

the  $N_2$  flow was increased from 0 to 550  $cm^3/min.$  In Figure 5, ternary diagram indicates with a solid line the expected compositions ranging between  $Si_3N_4$  and  $SiO_2$  if  $SiO_xN_y$  is a pseudo-binary mixture of  $Si_3N_4$  and  $SiO_2$ . The data shows the composition of the first series of films produced. The slight deficiency of Si in our films compared to the pseudo-binary is consistent with the results of others.<sup>9</sup> The composition was determined by depositing the films on Si substrates that had previously been coated with pyrolytic carbon and then performing 2 MeV RBS measurements. The carbon films were thick enough to shift the portion of the spectrum due to the Si substrate to energies well below those of the N and O peaks so that the composition could be determined more accurately.

The same series of  $SiO_xN_y$  films was simultaneously deposited on clean <100> Si substrates, and the substrates were subsequently annealed under liquid Ga at  $800^\circ C$  for 30 min. The samples coated with  $Si_3N_4$  or with  $SiO_xN_y$  containing 21 or 28 at.% O did not survive the anneal. Portions of RBS spectra of the remaining samples showing the relative amounts of Ga that diffused into the different films are shown in Figure 6. As the oxygen content of the films is increased, they become even less effective as a diffusion barrier to Ga than is  $SiO_2$ . The permeability of the films to Ga apparently increases with the oxygen concentration, but somewhere in the range of 46 to 66 at.% the solubility of Ga in the films begins to decrease. The  $SiO_2$  films used here were produced from silane and nitrous oxide at  $600^\circ C$  rather than from silane and oxygen at  $390^\circ C$ , as in our usual silox process.

In Figure 7, RBS spectra are shown for a GaAs substrate capped with  $SiO_xN_y$  containing 47 at.% O and for a GaAs substrate capped with  $600^\circ C$   $SiO_2$ . Both were annealed in forming gas at  $800^\circ C$  for 30 min. The GaAs substrate edge is at a much lower energy in the case of the  $SiO_2$  film because that film was considerably thicker than the oxynitride. Much more out-diffusion occurs into the oxynitride than into the  $SiO_2$ , which is consistent with the results of the in-diffusion experiments. The assumption that the diffusing species is Ga based on previous work.<sup>10</sup> This will be confirmed using Auger spectroscopy.

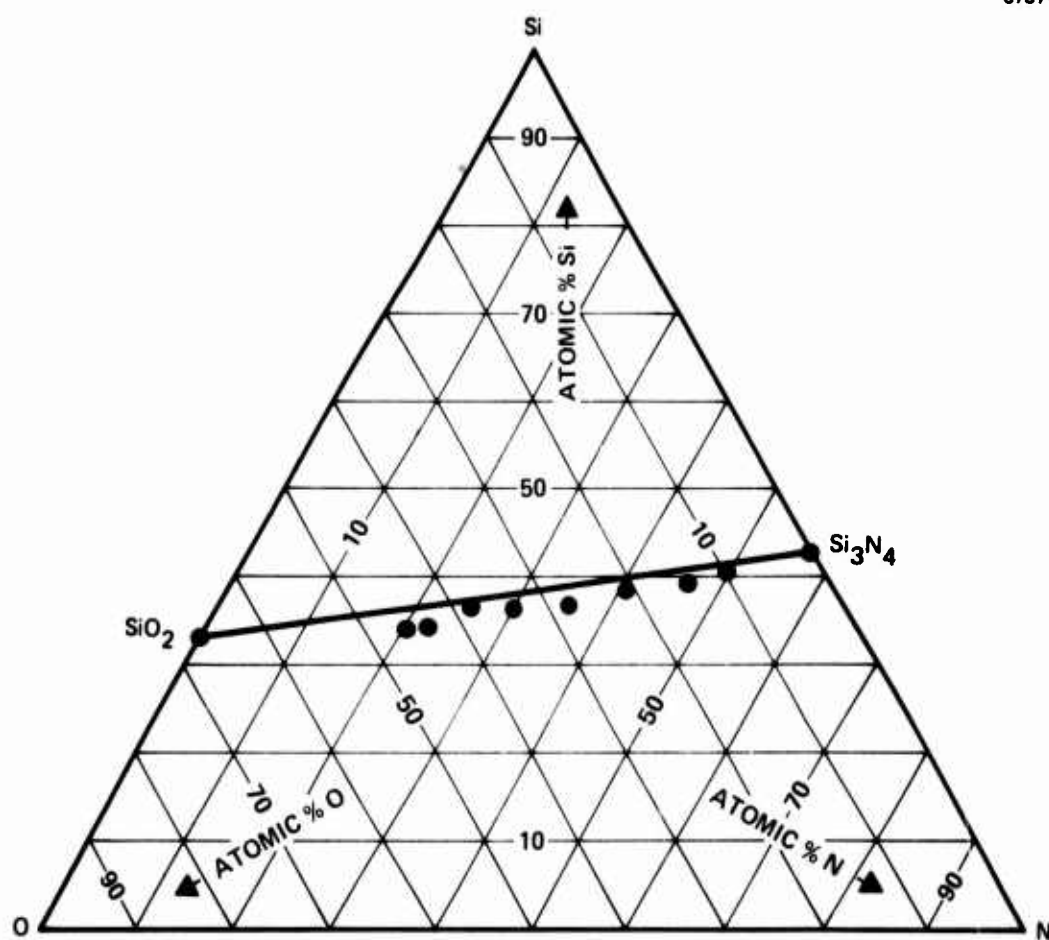


Figure 5. Composition of pyrolytic silicon oxynitrides deposited at 600°C using silane, ammonia, and nitrous oxide (nitrogen carrier).

6787-3

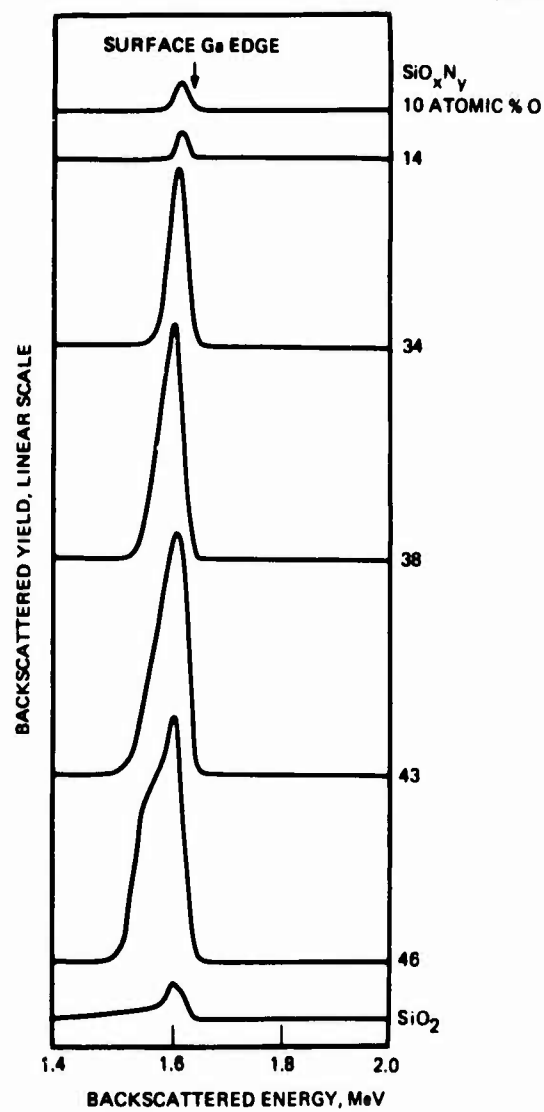


Figure 6. Gallium diffusion into  $\text{SiO}_x\text{Ny}$  and  $\text{SiO}_2$  films deposited at 600°C. The curves show only the portion of the 2MeV  ${}^4\text{He}^+$  backscattering spectra caused by Ga in the deposited films.

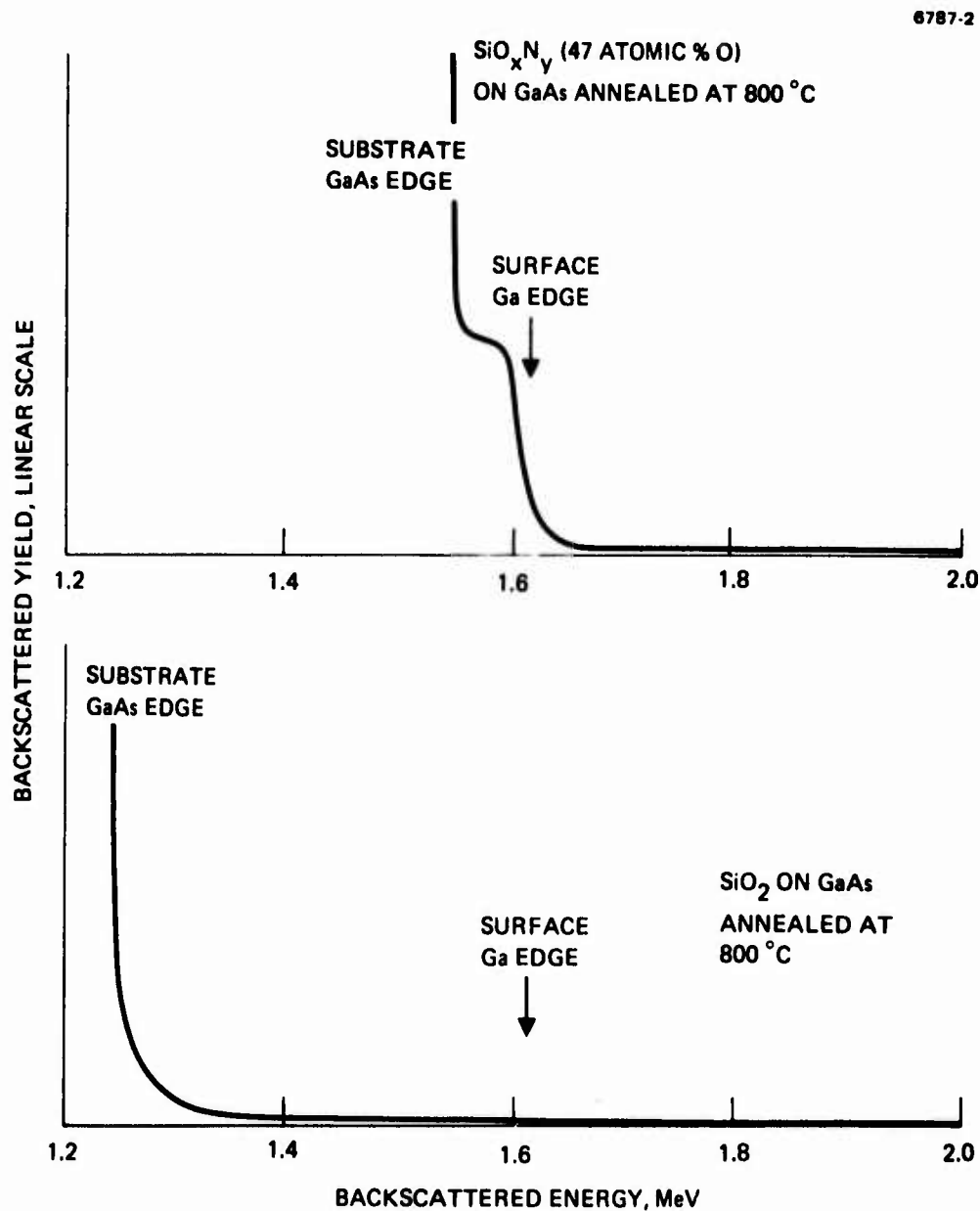


Figure 7. Comparison of Ga out-diffusion from GaAs as determined by 2MeV  ${}^4\text{He}^+$  backscattering measurements.

Another series of films ranging in composition from  $\text{Si}_3\text{N}_4$  to  $\text{SiO}_2$  has been deposited on samples of Si, carbon-coated Si, and GaAs. RBS determination of the composition of each film is complete, and the Ga out-diffusion from a set of GaAs substrates annealed at  $800^\circ\text{C}$  for 30 min is being measured. Table 5 gives the physical appearance of a set of GaAs samples that were annealed at  $900^\circ\text{C}$  for 30 min in cleaned argon. Examining the samples under a dark field microscope showed that films of  $\text{Si}_3\text{N}_4$  and oxynitride containing up to 9 at. % O exhibited cracking, while films containing 21 to 47 at. % O were either blistered or contained many bubbles or defects visible at low magnification. Only the  $600^\circ\text{C}$   $\text{SiO}_2$  film appeared free of significant damage; it contained only a few very small bubbles or precipitates.

Table 5. Physical Appearance of Encapsulated GaAs Samples after a  $900^\circ\text{C}$ , 30-min Anneal

Atomic % O	Appearance
0 ( $\text{Si}_3\text{N}_4$ )	cracked
7	cracked
9	cracked
21	intact but contains many defects
30	intact but contains many defects
36	intact but contains many defects
43	blistered
45	blistered
45	blistered
47	blistered
66 ( $\text{SiO}_2$ )	small number of bubbles, or precipitates.

Our most recent evaluations of encapsulant effects on the electrical properties of ion-implanted layers have employed selenium implants into two semi-insulating (Cr-doped) ingots. All dice described here were provided with implanted corner contact pads ( $5 \times 10^{13}$  200 keV Se<sup>+</sup>/cm<sup>2</sup> implanted at room temperature). Some dice were reserved for use as control samples and were not implanted further. The remaining dice were then given an over-all implant of  $1 \times 10^{13}$  260 keV Se<sup>+</sup>/cm<sup>2</sup> at room temperature or at 250°C. The dice were then annealed in sets. These sets generally contained both implanted and control samples. Following annealing, the encapsulant was removed with HF, and In-Ag-Ge contacts were soldered to the corner area. Hall-resistivity measurements were made on all dice. Results from a few dice that exhibited excessive drift in their measured values are not included.

Tables 6 and 7 summarize the electrical measurements on these ion/substrate combinations. Because of degeneracy effects, the measurable donor concentration is not necessarily a quantitative representation of the actual number of active donors present.<sup>11</sup> Assuming a Gaussian distribution of implanted ions, the dose/energy parameters used would result in only 40% of the implanted ions being detected as donors by Hall-effect measurements even if all of the ions were made electrically active. If implant channeling and/or diffusion broaden the implanted profile, a greater activation could be measured, but only where sufficient ion movement has occurred to reduce the peak concentration substantially from the theoretical starting value of  $10^{18}$ /cm<sup>3</sup>.

Observed donor activation greater than 100% has been attributed elsewhere to the encapsulant deposition parameters.<sup>3</sup> Table 6 shows that greater than 100% donor activation follows higher temperature anneals, even given an allowance for the presence of conductive skin (as evidenced by data from the control samples). At 800°C, the various batches of silicon dioxide have essentially the same effects on the two ingots examined and comparisons of the other films at this anneal temperature seem justified. Encapsulant parameters were not compared for anneal temperatures greater than 800°C. Data from samples given a proprietary capless anneal is included as reference for this ingot.

Table 6. Summary of Anneal Studies on GaAs Ingots #3106  
 Implant:  $10^{13}$  260 keV Se<sup>+</sup>/cm<sup>2</sup> at Room Temperature or 250°C.

Encapsulant	Number of Dice	Sheet Resistivity, Ω/□	Hall Electron Mobility, cm <sup>2</sup> /Vsec	Sheet Electron Concentration, cm <sup>-2</sup>	Anneal Temperature, °C
Implanted at room temperature:					
None <sup>a</sup>	2	444 ± 39 6.5 × 10 <sup>5</sup>	3420 ± 50 -36.30	(4.14 ± 0.42) × 10 <sup>12</sup> -2.6 × 10 <sup>11</sup>	800
Control	1				800
Low temperature oxide I	2	537 ± 38 none	3230 ± 100	(3.62 ± 0.36) × 10 <sup>12</sup>	800
Control	0				800
Low temperature oxide I	1	222.7 none	3073	9.12 × 10 <sup>12</sup>	850
Control	0				850
Low temperature oxide I	1	106.4 503.1	3404 2678	1.72 × 10 <sup>13</sup> 4.63 × 10 <sup>12</sup>	900
Control	1				900
Implanted at 250°C:					
None <sup>a</sup>	2	231 ± 29 5.3 × 10 <sup>7</sup>	3780 ± 420 177.5	(7.22 ± 0.12) × 10 <sup>12</sup> 6.7 × 10 <sup>8</sup>	800
Control	1				800
Low temperature oxide I	2	282 ± 18 none	3770 ± 40	(5.89 ± 0.32) × 10 <sup>12</sup>	800
Control	0				800
Low temperature oxide I	1	171.3 none	3225	1.13 × 10 <sup>13</sup>	850
Control	0				850
Low temperature oxide I	1	85.64 182.4	3191 3268	2.28 × 10 <sup>13</sup> 1.05 × 10 <sup>13</sup>	900
Control	1				900

<sup>a</sup>Capless anneal.

TABLE 7. SUMMARY OF ENCAPSULANT STUDIES ON GaAs INGOT #2988  
 Implant:  $1 \times 10^{13}$  260 keV Se<sup>+</sup> /cm<sup>2</sup> at room temperature. 800°C, 30-min anneal.

Encapsulant	Number of Samples	Sheet Resistivity, Ω/□	Hall Electron Mobility, cm <sup>2</sup> /V-sec	Sheet Electron Concentration, cm <sup>-2</sup>
Low temperature oxide I Control	4 2	454 ± 32 1520 ± 175	3360 ± 370 4036 ± 93	(4.10 ± 0.18) × 10 <sup>12</sup> (1.03 ± 0.14) × 10 <sup>12</sup>
Low temperature oxide II Control	4 2	402 ± 40 982 ± 162	3206 ± 353 4135 ± 211	(4.88 ± 0.17) × 10 <sup>12</sup> (1.57 ± 0.34) × 10 <sup>12</sup>
High temperature oxide Control	4 1	480 ± 260 -7 × 10 <sup>5</sup>	3173 ± 1159 5280	(4.77 ± 0.47) × 10 <sup>12</sup> 1.5 × 10 <sup>11</sup>
High temperature oxide blended to nitride and back to oxide Control	4 2	488 ± 18 (1.8 ± 0.85) × 10 <sup>8</sup>	3593 ± 63 198.4 ± 38	(3.56 ± 0.12) × 10 <sup>12</sup> (1.87 ± 0.53) × 10 <sup>8</sup>
Thin high temperature oxide overcoated with thick nitride Control	2 2	(1.9 ± 1.1) × 10 <sup>8</sup> (1.69 ± 0.5) × 10 <sup>8</sup>	106.2 ± 58 164.4 ± 53	(5.0 ± 4.9) × 10 <sup>8</sup> (2.59 ± 1.5) × 10 <sup>8</sup>
Thin high temperature oxide overcoated with thin nitride and oxide Control	4 1	478 ± 37 8.05 × 10 <sup>8</sup>	3107 ± 329 49.34	(4.24 ± 0.31) × 10 <sup>12</sup> 1.57 × 10 <sup>8</sup>
Oxynitride (25% O) overcoated with high-temperature oxide Control	4 1	(3.1 ± 3.7) × 10 <sup>4</sup> 7.20 × 10 <sup>7</sup>	1526 ± 131 -1.073	(3.2 ± 1.2) × 10 <sup>12</sup> -8.08 × 10 <sup>10</sup>
Oxynitride (15% O) overcoated with high-temperature oxide Control	2 1	(1.5 ± 1.8) × 10 <sup>4</sup> 2.02 × 10 <sup>7</sup>	580.0 ± 734 -10.52	(3.46 ± 0.22) × 10 <sup>12</sup> -293 × 10 <sup>10</sup>
Thin nitride overcoated with high-temperature oxide Control	3 2	1030 ± 260 (5.66 ± 1.2) × 10 <sup>8</sup>	2370 ± 670 681.6 ± 76.3	(2.7 ± 0.1) × 10 <sup>12</sup> (1.65 ± 0.18) × 10 <sup>7</sup>
Thin nitride only Control	4 1	(1.4 ± 0.9) × 10 <sup>4</sup> 6.06 × 10 <sup>7</sup>	144 ± 193 14.25	(4.6 ± 3.0) × 10 <sup>12</sup> (much drift) 7.12 × 10 <sup>9</sup>
Thick nitride only Control	4 2	(4.4 ± 4.0) × 10 <sup>8</sup> (13.6 ± 6.0) × 10 <sup>8</sup>	91 ± 77 238 ± 68	(1.3 ± 1.7) × 10 <sup>9</sup> (much drift) (2.4 ± 1.6) × 10 <sup>7</sup>

Tables 6 and 7 show that dice encapsulated with an oxide interface and that lack a thick nitride film will exhibit similar characteristics regardless of the method used to deposit that film and the ingot examined. The dice coated with oxynitrides had lower carrier mobility; the stoichiometric 600<sup>0</sup>C Si<sub>3</sub>N<sub>4</sub> used further depressed the measured mobility and produced visible strain in the dice surfaces. Capless annealing produced data in good agreement with that obtained with oxide encapsulants. The measurements of these dice show 40% apparent activation, which is in good agreement with the Gibbons and Tremain argument<sup>4</sup> and indicates that little spreading has occurred. Dice with the same annealing conditions which had been implanted at 250<sup>0</sup>C exhibited 70% apparent activation (Table 6) and a drop in peak carrier concentration to about 10<sup>17</sup>/cm<sup>3</sup> (assuming 100% actual activation).

The variations in Ga vacancy concentration indicated by the significant differences in the amount of Ga detected in the encapsulant film following 800<sup>0</sup>C annealing would be expected to affect the electrical measurements, but no effects were found. No correlation was found between the electrical measurements and the permeability of the encapsulant film to Ga. The mechanical stress inherent in the Si<sub>3</sub>N<sub>4</sub> used has outweighed any advantages from its lower permeability to Ga.

These results appear to contradict those of the MIT Lincoln Labs group,<sup>1</sup> who have had good success with pyrolytic silicon nitride. But one of their investigators, however, recently disclosed that the deposition parameters used at Lincoln Labs are significantly different from those used at HRL. In particular, the best results at Lincoln Labs resulted when gas mixtures were used that have ammonia concentrations far above those we have been using. Silicon nitride deposited under these conditions may have lower stress or higher plasticity than the films we have been using. We will evaluate films of this type early in the next contract period.

### SECTION 3

#### SULFUR TRANSFER TEST S 1

In cooperation with Code 5212, NRL, we tested the transferability of ion implantation of sulfur into GaAs using plasma-deposited  $\text{Si}_3\text{N}_4$  as an annealing cap. This section summarizes the results of this test. A more complete discussion is provided in Ref. 2. As in the beryllium implantation transfer test described in a previous progress report,<sup>12</sup> complete sets of test dice were to be processed independently at both HRL and NRL. At the time of these experiments, however, neither facility was equipped to deposit reliable  $\text{Si}_3\text{N}_4$  films. At that time, Dr. Adir Jacob of LFE Corporation, Waltham, Massachusetts, volunteered to prepare plasma-deposited  $\text{Si}_3\text{N}_4$  films on samples from both laboratories. We therefore decided to compromise the total separation of the samples from the two laboratories by using encapsulant films from a single source. We wish to thank Dr. Jacob for supplying the encapsulant films and Mr. William Uchytil of Metro-Line Western, Inc., Anaheim, California, for arranging to have the coatings prepared.

Before the samples were shipped to Dr. Jacob, all the dice were chemically cleaned at HRL. The  $\text{Si}_3\text{N}_4$  films were deposited only on the implanted side of the test dice. To protect against degradation of the edges of the samples during annealing, all dice were coated on both sides with  $\sim 2000 \text{ \AA}$  of pyrolytic  $\text{SiO}_2$  at HRL before further processing. Thus, this transfer test represents a test of the transferability of the implantation and annealing procedures employed, but not of the ability of the two laboratories to prepare functionally identical  $\text{Si}_3\text{N}_4$  coatings. The complete processing sequence used is detailed in Table 8.

To assess the consistency of the electrical evaluation techniques at our two facilities, all the samples were tested for sheet resistivity  $R_s (\Omega/\square)$  and Hall-effect mobility  $\mu_H (\text{cm}^2 \text{V}^{-1} \text{S}^{-1})$  at both laboratories. The results of these measurements are presented in Table 9.

Statistical analysis of the electrical data was performed to determine if systematic differences existed between the samples prepared

Table 8. Implant Processing for Sulfur Transfer Test S1

Step	Description
1	Ninety-eight dice from Crystal Specialties ingot No. 3106, numbered between 1 and 100, sent to NRL. 99 dice, numbered 101 to 199, used at HRL. All dice cleaved from slices No. 13 through No. 18 and roughly 7 mm x 7 mm x 0.3 mm.
2	Dice implanted in sets of four (four dice = 1 batch). Two control dice processed with each batch and shielded from implantation by masking.
3	Pre-implant cleaning: <ul style="list-style-type: none"> <li>(a) Heat in TCE to bubbling</li> <li>(b) Flush, thoroughly rinse, then heat to bubbling in methanol</li> <li>(c) Flush and thoroughly rinse in deionized water</li> <li>(d) Soak in HF 1 minute</li> <li>(e) Rinse thoroughly in deionized water</li> <li>(f) Blow dry with filtered boil-off nitrogen.</li> </ul>
4	Two batches implanted with $5.6 \times 10^{13} \text{ cm}^{-2}$ 120 keV S <sup>+</sup> at room temperature.
5	Two batches implanted with $5.6 \times 10^{13} \text{ cm}^{-2}$ 120 keV S <sup>+</sup> at 250°C.
6	All samples implanted with corner contacts <ul style="list-style-type: none"> <li>(a) Masks heavy aluminum foil, revealing quarter-circle in each corner of sample, radius of quarter-circle ~1/16 in.</li> <li>(b) Dose <math>5 \times 10^{14} \text{ cm}^{-2}</math> 20 keV S<sup>+</sup>, <math>5 \times 10^{14} \text{ cm}^{-2}</math> 140 keV S<sup>+</sup>, both at room temperature.</li> </ul>
7	Repeat steps 3(a), 3(b), and 3(f).
8	Step 7 repeated at HRL.
9	Samples coated with roughly 2000 Å Si <sub>3</sub> N <sub>4</sub> at LFE Corporation (implanted side only)
10	Samples coated on both sides with roughly 2000 Å of pyrolytic SiO <sub>2</sub> at HRL. Annealing performed in flowing forming gas (15% H <sub>2</sub> , 85% N <sub>2</sub> ).
11	Anneal time 30 minutes. All glassware in hot zone of furnace is Spectrosil synthetic quartz. One batch from each of steps 4 and 5 annealed at 800°C. One batch from each of steps 4 and 5 annealed at 900°C.
12	Remove encapsulant by soaking in HF. Quench and rinse thoroughly in DIW. Blow dry with filtered dry nitrogen gas.
13	Corner contacts soldered on using In-Ag-Ge solder prepared as follows: <ul style="list-style-type: none"> <li>(a) Cover most of one surface of a Ge wafer with 90:10 In:Ag solder (Indalloy No. 3)</li> <li>(b) Anneal in argon at 600°C until melt forms into a smooth-surfaced mass</li> </ul>
14	Soldering performed using a fine-tipped soldering pencil. Solder alloy is simply picked off of surface of Ge wafer with soldering tip. Contacts kept as small as possible consistent with requirements of Hall measurement apparatus. Sinter contacts if necessary in forming gas for 30 sec at 300°C.

2160

Table 9. Composite Results from Sulfur Transfer Test "S1"  
 Statistics: 90% Confidence Limits on Mean Values of Measured Variables

Implant Temperature, °C	Anneal Temperature, °C	Parameter: $R_S (\Omega/\square)$ or $\mu_H (cm^2 V^{-1} s^{-1})$	Prepared at Lab A		Prepared at Lab B	
			N <sup>*</sup>	Lab A	Lab B	N <sup>*</sup>
20 (Nominal)	800	$R_S$	3 (4)	252 ± 28 234 ± 46	253 ± 27 256 ± 17	2 3 <sup>r</sup>
		$\mu_H$	3 (4)	<sup>s</sup> 3080 ± 100 3420 ± 790	3240 ± 190 3210 ± 140	2 3 <sup>r</sup>
	900	$R_S$	2	82.8 ± 0.1	<sup>m</sup> 84.2 ± 0.6 <sup>†</sup>	3
		$\mu_H$	2	2720 ± 190	2870 ± 470	3
	250	$R_S$	3 <sup>r</sup> (4 <sup>r</sup> )	92.8 ± 4.7 94.9 ± 5.5	<sup>s</sup> 93.7 ± 2.0 121 ± 64 <sup>■</sup>	3 4
		$\mu_H$	3 <sup>r</sup> (4 <sup>r</sup> )	3730 ± 210 3700 ± 140	3870 ± 170 3400 ± 1200 <sup>■</sup>	3 4
900	800	$R_S$	3 <sup>r</sup> (4 <sup>r</sup> )	<sup>m</sup> 69.1 ± 6.7 70.7 ± 5.3	<sup>m</sup> 70.3 ± 5.2 --	3470 ± 80 --
		$\mu_H$	4 <sup>r</sup>	<sup>s</sup> 3340 ± 40 3380 ± 100	<sup>m</sup> 3440 ± 80 --	90 ± 13 --
						3580 ± 260 3900 ± 140

\* Number of samples. Superscript "r" denotes that one or more of the samples in the data set has a four-terminal resistance ratio greater than 3.0. Parentheses indicate that a measurement of one sample at one facility is questionable by inspection.

† Lab A and Lab B mean value limits on same samples do not overlap.

■ Lab A and Lab B values for measurements on same samples do not pass F test for standard deviations at 90% confidence level.

<sup>m</sup> Mean value limits for samples prepared at Lab A and Lab B (measured at same facility) do not overlap.

<sup>s</sup> Measurements at same facility on samples prepared at Lab A and Lab B do not pass F test for standard deviations at 90% confidence level.

at the two facilities or between the measurements compiled at the two locations. The analysis used was described in detail in Ref. 2.

Transferability was assessed for 14 pairs of data sets: 6 for samples implanted at room temperature and 8 for samples implanted at 250°C. Of the 6 pairs of room-temperature data, one pair failed to pass our criterion for consistency of mean value, and another failed our test for consistency of dispersion. These results indicate that, for samples implanted at room temperature and annealed at either 800°C or 900°C, the process sequence used is transferable. On the other hand, of the 8 pairs of data for 250°C implants, there were three failures of the mean value test and two failures of the dispersion test. All three values of the mean value test occurred for samples annealed at 900°C. Thus, there is a clear failure to achieve transferability for implantation at 250°C with annealing at 900°C. On the other hand, implantation at 250°C followed by annealing at 800°C appears to be transferable.

Twenty pairs of data sets were compared for measurement consistency. Two pairs failed our test for consistency of mean values and two pairs failed the test for dispersion. This failure rate is consistent with normal statistical fluctuations of the measurements and indicates that there are no significant systematic differences between the measurements at the two facilities for tests involving few samples sets.

On the basis of these results, we conclude that the implantation and annealing process sequence that we have used is transferable for 20°C implantation followed by 800°C or 900°C annealing and for 250°C implantation followed by 800°C annealing. A failure of transferability was observed for 250°C implantation with 900°C annealing. These experiments were performed using plasma-deposited Si<sub>3</sub>N<sub>4</sub> prepared by an outside source. Thus, this transfer test does not reflect the ability of our two laboratories to prepare functionally equivalent encapsulant films. Further experiments will be performed to answer this question.

Table 10 gives some indication of our ability to produce electrically active layers of high quality. The layers produced by room-temperature implantation followed by 800°C annealing were decidedly inferior to all the other layers. The remaining layers are roughly three times lower in sheet resistivity than those implanted at room temperature and

Table 10. Results for Four Implant Conditions Using Pyrolytic  $\text{SiO}_2$  Encapsulation and  
 $800^{\circ}\text{C}$ , 30-min Anneals in Argon

Implanted Species	Fluence of Each Species, $\text{cm}^{-2}$	No. of Samples	Sheet Resistivity, $\Omega/\square$	Hall Electron Mobility, $\text{cm}^2\text{V}^{-1}\text{s}^{-1}$	Apparent Electrical Activity, %
S + Ga	$10^{13}$	4	420 $\pm 68$	3730 $\pm 100$	44.1 $\pm 5.5$
	$10^{13}$	3	387 $\pm 55$	3740 $\pm 76$	41.4 $\pm 5.3$
S + Ga	$10^{14}$	2	105 $\pm 10$	3390 $\pm 70$	17.7 $\pm 2.1$
	$10^{14}$	3	119 $\pm 9$	3260 $\pm 11$	16.1 $\pm 1.2$
Se + Ga	$10^{13}$	3	395 $\pm 34$	3290 $\pm 450$	48.8 $\pm 5.1$
	$10^{13}$	2	371 $\pm 36$	3630 $\pm 40$	46.6 $\pm 4.9$
Se + Ga	$10^{14}$	4	220 $\pm 43$	2777 $\pm 83$	10.4 $\pm 1.8$
	$10^{14}$	4	145 $\pm 10$	2998 $\pm 52$	14.4 $\pm 1.1$

5983

annealed at 800<sup>o</sup>C. In terms of carrier mobility, all the samples implanted at 250<sup>o</sup>C are definitely superior to those implanted at 20<sup>o</sup>C and annealed at 900<sup>o</sup>C. Of those implanted at 250<sup>o</sup>C, the samples annealed at 900<sup>o</sup>C have lower sheet resistivities than samples from the same facility but annealed at 800<sup>o</sup>C. No clear conclusion can be drawn concerning the relative mobilities obtained at the two anneal temperatures, however. Thus it is clear that better overall results were obtained from the samples implanted at 250<sup>o</sup>C. Considering the apparent transferability failure observed for 250<sup>o</sup>C implantation with 900<sup>o</sup>C anneals, the results obtained from this transfer test indicate that the best choice for obtaining reproducible layers of high quality from this process sequence is to implant at 250<sup>o</sup>C and anneal at 800<sup>o</sup>C.

SECTION 4  
DUAL IMPLANTATION

Using dual implantation techniques, we were able to increase the relative activation efficiency of selenium donors by 40% at a dose of  $10^{14} \text{ cm}^{-2}$  (Ref. 4). Table 10 summarizes our results for four implant conditions using pyrolytic  $\text{SiO}_2$  encapsulation and  $800^\circ\text{C}$ , 30-min anneals in argon. These results were obtained from implants performed at elevated temperature ( $200$  or  $250^\circ\text{C}$ ) and at random incidence ( $7^\circ$  tilt) into bare GaAs substrates from Crystal Specialties ingot 2988. Dual implants, where used, were performed first and were spatially matched to the donor implant (projected ranges were matched; standard deviations of projected range agree within a few percent). The sulfur implants were performed at 100 keV and dual implants of Ga at 300 keV. Selenium implants were performed at 220 keV with dual implants at 200 keV. The values obtained for the selenium implants at  $10^{14} \text{ cm}^{-2}$  are in good agreement with the results reported by Woodcock<sup>12</sup> using CVD "silicon nitride" encapsulation.

These results show clearly that dual implantation with sulfur (under the conditions studied) has no significant effect other than to reduce slightly the scatter in the data (as had been observed in our previous studies). In contrast, dual implantation does significantly affect the electrical activity of selenium at the higher dose studied. Our hypothesis is that neither hot implantation nor  $800^\circ\text{C}$  annealing by itself is sufficient to cause strong gallium-site occupation by implanted gallium atoms, but that the lattice disruption caused by the hot selenium implant performed after the gallium implant provides sufficient steady-state disorder to encourage preferential lattice-site location by both the selenium and gallium implants. Dual implantation will be effective only if both implants exhibit strong lattice-site preference. Sulfur implantation after gallium implantation is ineffective presumably because insufficient disruption occurs during the implantation process. If this is true, additional damage generation following the gallium implant (e.g., by proton or alpha-particle bombardment) should cause enhanced electrical

activity of sulfur implants in conjunction with gallium dual implantation. Alternatively, gallium implantation following sulfur implantation may be effective. Doping profile alteration under all dual implantation conditions is to be expected.

## SECTION 5

### STUDIES OF THE THERMAL CONVERSION OF SEMI-INSULATING GaAs

During this contract period, we analyzed two samples of high-purity, semi-insulating LEC GaAs and one sample of Varian semi-insulating GaAs (all supplied by Code 5221, NRL) plus an unidentified wafer of semi-insulating GaAs supplied by Code 5211, NRL. All of these samples exhibited p-type conversion under our standard test procedure (2-hr anneal at  $\sim 800^{\circ}\text{C}$  in a liquid-tight container submerged in a Ga melt saturated with GaAs). The container is readily permeated by the vapors from the melt, which provide an equilibrating ambient to prevent surface decomposition of the wafer). Both n- and p-type conversions have been observed under this test procedure.

The two LEC samples (from ingots II-40L and II-22) and the Varian wafer exhibited mild p-type conversion, having sheet carrier concentrations (after annealing) of  $4 \times 10^{11}$ ,  $2 \times 10^{11}$ , and  $4 \times 10^{11} \text{ cm}^{-2}$ , respectively, with corresponding Hall mobilities (for holes) of 230, 68, and  $328 \text{ cm}^2\text{V}^{-1}\text{s}^{-1}$ . Stripping measurements on the sample from ingot II-40L indicated that most of the electrical activity was confined to the outer 3000 Å of material, but p-type conductivity persisted even after removal of 1.2  $\mu\text{m}$  of material. Stripping of the other two substrates gave inconclusive results.

The unidentified wafer from Code 5211, NRL, exhibited extremely strong p-type conversion. After our 2-hr test, this material exhibited a sheet carrier concentration of  $9.4 \times 10^{13} \text{ cm}^{-2}$  with a Hall mobility of  $259 \text{ cm}^2\text{V}^{-1}\text{s}^{-1}$ . No stripping was performed on this sample.

#### REFERENCES

1. C.O. Bozler, J.P. Donnelly, R.A. Murphy, R.W. Laton, R.W. Sudbury, and W.T. Lindley, *Appl. Phys. Lett.* 29, 123 (1976).
2. Semi-Annual Progress Report No. 1, This Contract, April, 1977.
3. E.A. Irene, *J. Electronic Materials* 5, 287 (1976).
4. Quarterly Technical Report No. 2, This Contract, August 1977.
5. R. Lathlaen and D.A. Diehl, *J. Electrochem. Soc.* 116, 620 (1969).
6. W. Kern, G.L. Schnable, and A.W. Fisher, *RCA Review* 37, 3 (1976).
7. N.C. Tombs, F.A. Sewell, Jr., and J.J. Comer, *J. Electrochem. Soc.* 116, 869 (1969).
8. N.C. Tombs, U.S. Patent 3,422,321 (1969).
9. M.J. Rand and J.F. Roberts, *J. Electrochem. Soc.* 120, 446 (1973).
10. J. Gyulai, J.W. Mayer, I.V. Mitchell and V. Rodriguez, *Appl. Phys. Lett.* 17, 332 (1970).
11. J.F. Gibbons and R.E. Tremain, Jr., *Appl. Phys. Lett.* 26, 199 (1975).
12. Quarterly Progress Report No. 1, This Contract, 1 October 1976 through 31 December 1976.